International Journal of Engineering Trends and Technology
ISSN: 2231–5381 / https://doi.org/10.14445/22315381/IJETT-V71I8P213

Volume 71 Issue 8, 152-160, August 2023

Original Article

Robust Human Activity Recognition using Improved Heuristic Search Algorithm with Deep Autoencoder Model

L. Maria Anthony Kumar[1], S. Murugan[2]

[1]*Department of Computer and Information Science, Annamalai University, Annamalai Nagar, Tamil Nadu, India.*
[2]*Dr. M.G.R. Government Arts and Science College for Women, Villupuram, Tamil Nadu, India.*

[1]*Corresponding Author : lmakumarphd@gmail.com*

Received: 10 April 2023 Revised: 10 June 2023 Accepted: 05 August 2023 Published: 15 August 2023

Abstract *- Human Activity Recognition (HAR) by employing smart home sensors is a topic that is undergoing intense research in the area of ambient-supported living and the basis of ubiquitous computing in smart environments. Recently, HAR majorly utilizes Deep Learning (DL) method since they employ representation learning methods that could automatically produce maximum factors from raw input datasets resulting from the sensor in the absence of human interference and could detect Hidden Layer (HL) patterns in a dataset. The study presents an Improved Manta-Ray Foraging Optimization with Deep Autoencoder (IMRFO-DAE) model for HAR. The presented algorithm majorly recognizes the diverse types of human activities. The presented IMRFO-DAE model pre-processes the human activity data via a standardization approach to obtain this. Next, the IMRFO-DAE method uses the DAE model to perform the Activity Recognition (AR) process. To advance the AR accomplishment of the DAE model, the IMRFO method is applied as a hyperparameter optimizer. Moreover, the IMRFO model is derived by modifying the initialization of the MRFO model by implementing the chaotic concept. An extensive range of simulations was performed to depict the enhanced efficiency of the IMRFO-DAE approach. The simulation results assured the improved outcomes of the IMRFO-DAE approach compared to existing approaches.*

Keywords *- Human activity recognition, Deep learning, Metaheuristics, MRFO algorithm, Chaotic concept.*

1. Introduction

HAR has become an active research area for a few years because it is applicable in various fields and the rising need for convenience services and home automation for older people [1, 2]. Of these, AR in Smart Homes, by using ubiquitous and simple sensors, has grabbed more interest in the ambient intelligence domain and enabled present technologies to enhance the living standards of an individual within a home atmosphere [3]. The main objective of AR was to detect and find complex and simple activities in real-time settings utilizing sensor data. HAR has become an important research area because of its notable contributions in human-centric areas of a study intended to enhance the standard of life [4], contributes to the transportation, health, and safety in smart villages and smart cities, and assists policymakers to react efficiently to enhance the qualification of services. HAR structure offers data regarding the activity and behavior of the subjects [5, 6]. This can usually be attained by recording signals from smartphones or smart sensors and processing them using ML approaches for recognition [7]. HAR was used for continuous patient monitoring with different diseases, transportation, daily living activities, sports, and locomotion. As smart sensors will be the key new data sources, pattern recognition methods and Machine Learning (ML) established an excessive contribution to constitute smarter sensor applications [22]. Such methods have numerous techniques suitable for different regions. The data processing with ML approaches includes substantial data types like velocity, variety, and volume; data methods like unsupervised and supervised methods and using efficient approaches that suit the data features [9]. Since data can be produced by many sources with accurate data types, it is very significant to adopt or apply methods that manage the data features. Furthermore, finding the optimal data method suitable for the data was one of the critical phases for recognizing patterns and better analysing sensor data [10].

Dahou et al. [11] examine a new HAR method dependent upon optimized 2 techniques: CNN and a newly projected optimized technique, AOA, to boost HAR efficiency with some resources. The projected CNN was executed for learning and extracting features in input data, whereas an improved AOA approach, Binary AOA (BAOA), was utilized to select the most suitable features. Eventually, the SVM was applied

for classifying the Feature Selection (FS) dependent upon distinct performances. In [23], the 1D-CNN method is initially established betwixt supervised DL to an online HAR data classifier. For an automatic selection of a better hyperparameter of the CNN technique, 7 methods dependent upon meta-heuristic techniques are examined.

Fan and Gao [13] suggest integrating Bee Swarm Optimization (BSO) with Deep Q-networking (DQN) for carrying out FS and projecting a hybrid FS method, BAROQUE, in accordance with these 2 methods. Next wrapper system, BAROQUE leverages engaging properties in BSO and multi-agent DQN for determining feature subsets and implements a classification for evaluating these solutions. In BAROQUE, the BSO was utilized for striking a balance betwixt exploration as well as exploitation for searching of feature spaces, but the DQN gets benefits of the values of RL for making the local searching procedure further adaptive and more effective. In [14], a novel typical feature fusion and FS-based process were presented to automate HAR. The presented technique contains 3 basic stages optical flow-oriented motion section extracting and then ROI recognition, Gray Level Difference Matrix (GLDM), and shape feature is integrated into a single matrix dependent upon superiority value index, and eventually, Reyni Entropy Controlled Euclidean classification related optimum FS.

Al-Wesabi et al. [25] examine an Optimum DL-related HAR (ODL-HAR) technique on node-allowed IoT platforms. The presented system proposes to define human action in daily life utilizing wearable and IoT gadgets. The projected system utilizes the MobileNet_v2 approach as an extracting feature and the BiLSTM technique as a classification. For fine-tuning hyperparameters contained in BiLSTM approach optimum, Chaos Game Optimization (CGO) technique was utilized to enhance the detection efficiency. Helmi et al. [16] introduce an effective HAR method utilizing a lightweight FS system for enhancing the HAR classifier procedure. The established FS process, named GBOGWO, proposes to improve the efficiency of the Gradient Based Optimizer (GBO) technique by utilizing the GWO operator. Initially, the GBOGWO was utilized to select suitable features; afterwards, the SVM was utilized to classify the actions.

This article develops an Improved MantaRay Foraging Optimization with Deep Autoencoder (IMRFO-DAE) algorithm for HAR. The presented algorithm majorly recognizes the diverse types of human activities. The presented model pre-processes the human activity data via a standardization approach to obtain this. Next, the IMRFO-DAE method performs the AR process using the DAE algorithm. To enhance the AR performance of the DAE algorithm, the IMRFO model is applied as a hyperparameter optimizer. Moreover, the IMRFO approach is derived by modifying the initialization of the MRFO algorithm by utilizing the chaotic concept. A wide range of simulating procedures were accomplished to depict the precipitated achievement of the IMRFO-DAE approach.

2. The Proposed Model

The present research presents an innovative IMRFO-DAE approach for accurate HAR. The presented IMRFO-DAE approach majorly recognized the diverse classes of HARs. This has a three-state process: pre-processing, AR using DAE, and MRFO hyperparameter tuning. Fig. 1 demonstrates the workflow of the IMRFO-DAE system.

2.1. AR using DAE Model

Here, the IMRFO-DAE method performs the AR process using the DAE method. The presented approach is a feedforwarding neural network with more than one concealed layer. This is a kind of unsupervised NN wherein the network tries to match output to the input vector [24]. In addition, it is utilized for generating lower or higher dimensionality representations of inputted datasets. Using the unsupervised learning process of compressed info encoding will make NN extremely resourceful.

Additionally, this network is trained single layer at a time, which reduces the computation resource required to propose an efficient paradigm. If the hidden layer is lesser dimensional when compared to the input and output layers, then the network is utilized for encoding information (compression).

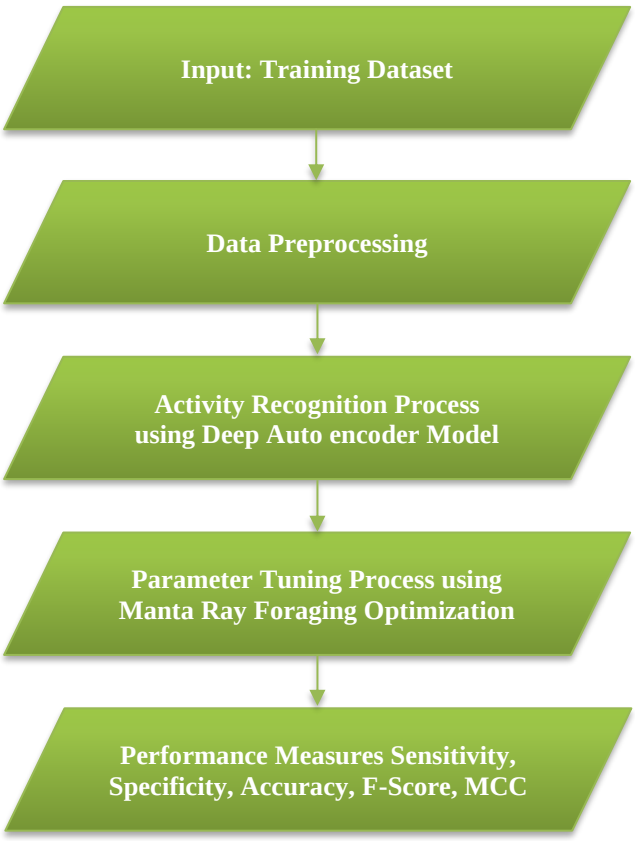

Fig. 1. Workflow of IMRFO-DAE system

Multi-layered AE is trained successively, which allows for the gradual compression of data, which creates what is named an SAE. The self-encoding models comprise output, input, and hidden layers:

$$\mathrm{x_i} = \left[\mathrm{x_{i1}}, \mathrm{x_{i2}}, \mathrm{x_{i3}}, \ldots, \mathrm{x_{ij}}\right]^T 154 \quad (1)$$

In the equation, i denotes $i\text{-}th$ flow table featuring vectors, and j characterizes every flow table featuring. The vector has $j\text{-}th$ featuring. The concealed layer will be encoding and compressing the input featuring vectors of the flow table based on the following expression:

$$\mathrm{encoder} = \mathrm{W_1 x_i} + \mathrm{b_1} \quad (2)$$

Now, W_1 indicates the weight connects the inputting and conceding layers, $\mathrm{x_i}$ refers to the input featuring vector of $i\text{-}th$ flow table, and b_1 represent the bias of concealed layers. Afterwards, the encoding process is finished and defined as the result of concealed layers. The resulting layer will be decoded and recreated to generate a result of a similar size as the inputting layer:

$$decoder = f(W_2(encoder)_i + b_2) \quad (3)$$

Where f represents the activation function, W_2 signifies the weighting value amid the inputting and conceding layers, $(encoder)_i$ characterize the stream table featuring vector compressed by the coding of the concealed layer, and b_2 shows the bias of outputting layer. Lastly, the self-encoding model can be accomplished by reducing the loss function:

$$loss = \sum_{i=1}^{N} (x_i - (decoder)_i)^2 \quad (4)$$

Whereas n denotes the flow table featuring vectors number, x_i indicate flow table featuring vector's input, and $(decoder)_i$ represent the outing value of the flow table featuring vectors by x_i.

2.2. Hyperparameter Tuning

To enhance the AR performance of the DAE model, the IMRFO algorithm is applied as a hyperparameter optimizer. MRFO is a recently proposed metaheuristic optimization technique which stimulates the foraging behavior of MR [18]. They have been evolving many different creative and impressive foraging strategies, namely somersault, chain, and cyclone foraging. They notice a higher abundance of plankton as the main goal (the better target solution) at the chain foraging phase. Then, they were combined together to constitute the foraging chain. Although every individual moves toward manta rays and food in front of them. The mathematical modelling for 3 foraging methods is discussed in the following:

2.2.1. Chain Foraging Technique

MRs could identify plankton and swim toward it. Consequently, the high concentration of the plankton was viewed as the highest destiny for MR and formed a forage chain through head-to-tail alignment to accomplish these configurations. Consequently, every individual is upgraded in all the iterations by a better solution. The foraging chain behaviors are arithmetically modelled in the following:

$$x_i^{t+1} = \begin{cases} x_i^t + r.(x_{best}^t - x_i^t) + \alpha(x_{b\theta jt}^t - x_i^t), i = 1 \\ x_i^t + r.(x_{i-1}^t - x_i^t) + \alpha(x_{\mathrm{best}}^t - x_i^t), i = 2{:}N \end{cases} \quad (5)$$

In Eq. (5), x_i^t indicates the i^{th} individual location for $t\text{-}th$ iteration; r signifies random vector; x_{best}^t shows the better solution for t^{th} iterations, N indicates the numbering of MR, and α indicates the weight co-efficient that is given below:

$$\alpha = 2 \times r \times \sqrt{|\log(r)|}. \quad (6)$$

2.2.2. Cyclone Foraging Technique

When a collection of MR identifies plankton in a deep watering process, they construct a longer forage chain and travel in a spiral toward food. Therefore, the said behavior is modelled scientifically to characterize the cyclone forage:

$$x_i^{t+1} = \begin{cases} x_{\mathrm{best}} + r.(x_{\mathrm{best}}^t - x_i^t) + \beta(x_{\mathrm{best}}^t - x_i^t), & i = 1 \\ x_{\mathrm{best}} + r.(x_{i-1}^t - x_i^t) + \beta(x_{\mathrm{best}}^t - x_i^t), & i = 2{:}N \end{cases} \quad (7)$$

In Eq. (7), β signifies a weight feature that is utilized in forming the spiral form, and it is computed in the following:

$$\beta = 2e^{r_1}\left(\frac{T - t + 1}{T}\right).\sin(2\pi r_1) \quad (8)$$

In Eq. (8), t signifies the existing iteration, T represents the maximal iteration count, and r_1 denotes a random value. The initial part of Eq. (7) illustrates the capability of MRFO to apply better solutions. But, to improve exploration probabilities, a random location through the search space is utilized as a reference location. Thus, the subsequent formula is applied in the exploration stage to attain a complete global search:

$$x_{rand} = Lb + r.(Ub - Lb), \quad (9)$$

$$x_i^{t+1} = \begin{cases} x_{rand} + r.(x_{rand}^t - x_i^t) + \beta(x_{rand}^t - x_i^t), & i = 1 \\ x_{rand} + r.(x_{i-1}^t - x_i^t) + \beta(x_{rand}^t - x_i^t), & i = 2{:}N \end{cases} \quad (10)$$

Whereas Ub and Lb denote upper and lower boundaries, and $xrand$ shows random points allocated to explore space.

2.2.3. Somersault Foraging Technique

The prey location is deemed as the pivot in this behavior. Everyone will swim around the pivot and somersault to a novel position. Consequently, they upgrade the position

according to the better location, and it is mathematically expressed in the following:

$$x_i^{t+1} = x_i^t + S.(r_2.-r_3.x_i^t), i = 1,2,N, \quad (11)$$

In Eq. (11), S indicates the somersault factors utilized for determining the somersault range of MR, whereas r_2 and r_3 shows the random number. Individual travels toward any location inside the searching region among the symmetrical and the current position around the food pivot. The procedure of transforming to an optimum resolution can be attained by reducing the distance between the position of manta rays and better location.

Thus, the somersault foraging range can be constrained in an adapting manner. In MRFO, the early population is distributed randomly, which could not assure the distribution of search agent space. Unpredictability and Ergodicity are the two characteristics of chaotic movement that could generate diversification in the early population:

$$x_{i+1} = sin\left(\frac{b\pi}{x_i}\right) \quad (12)$$

Whereas b is fixed as 0.7.

The IMRFO algorithm derives Fitness Functions (FFs) to achieve better classification precision. It sets a non-negative integer in characterizing the enhanced achievement of the candidate resolution. The reduced classification erroring rate can be considered FF.

$$fitness(x_i) = ClassifierErrorRate(x_i) = \frac{number\ of\ misclassified\ samples}{Total\ number\ of\ samples} * 100 \quad (13)$$

3. Result Analysis

The experimental validation of the IMRFO-DAE method is investigated by employing two datasets: UCI HAR [19], and USC HAD [20] datasets. Tables 1 and 2 represent the detailed description of the two datasets. Fig. 2 depicts some sample images.

Table 1. Description of the UCI HAR dataset

Label	Class	Sample Nos.
0	Walking	1722
1	Walking Upward	1544
2	Walking Downward	1406
3	Sitting	1777
4	Standing	1906
5	Lying	1944
Overall Samples		**10299**

Table 2. Description of the USC HAD dataset

Label	Class	Sample Nos.
0	Walking Left	70
1	Walking Downward	70
2	Running Toward Front	70
3	Standing	70
4	Sleeping	70
5	Elevating Upward	70
Overall Samples		**10299**

Fig. 2 Sample images

Table 3. HAR result of IMRFO-DAE model with distinct classes under UCI HAR dataset

Labels	$Accu_y$	$Sens_y$	$Spec_y$	F_{Score}	MCC
Training (70%)					
0	92.63	74.65	96.29	77.41	73.09
1	92.90	78.39	95.49	76.98	72.80
2	93.16	71.12	96.63	73.87	70.02
3	92.55	78.46	95.49	78.43	73.92
4	92.72	81.85	95.18	80.61	76.14
5	92.18	81.88	94.53	79.57	74.78
Average	**92.69**	**77.72**	**95.60**	**77.81**	**73.46**
Testing (30%)					
0	92.59	71.97	96.60	75.97	71.76
1	92.69	74.56	95.79	74.89	70.61
2	92.62	73.24	95.72	73.24	68.96
3	92.69	80.11	95.31	79.07	74.65
4	92.36	81.33	94.87	79.79	75.11
5	92.14	81.59	94.69	80.20	75.31
Average	**92.51**	**77.13**	**95.50**	**77.19**	**72.73**

The confusion matrix of the IMRFO-DAE approach to the HAR procedure is depicted in Fig. 3. The outputs denoted that the IMRFO-DAE algorithm has precisely recognized all six kinds of human activities.

Table 3 and Fig. 4 show comprehensive HAR results of the IMRFO-DAE model on the UCI HAR dataset.

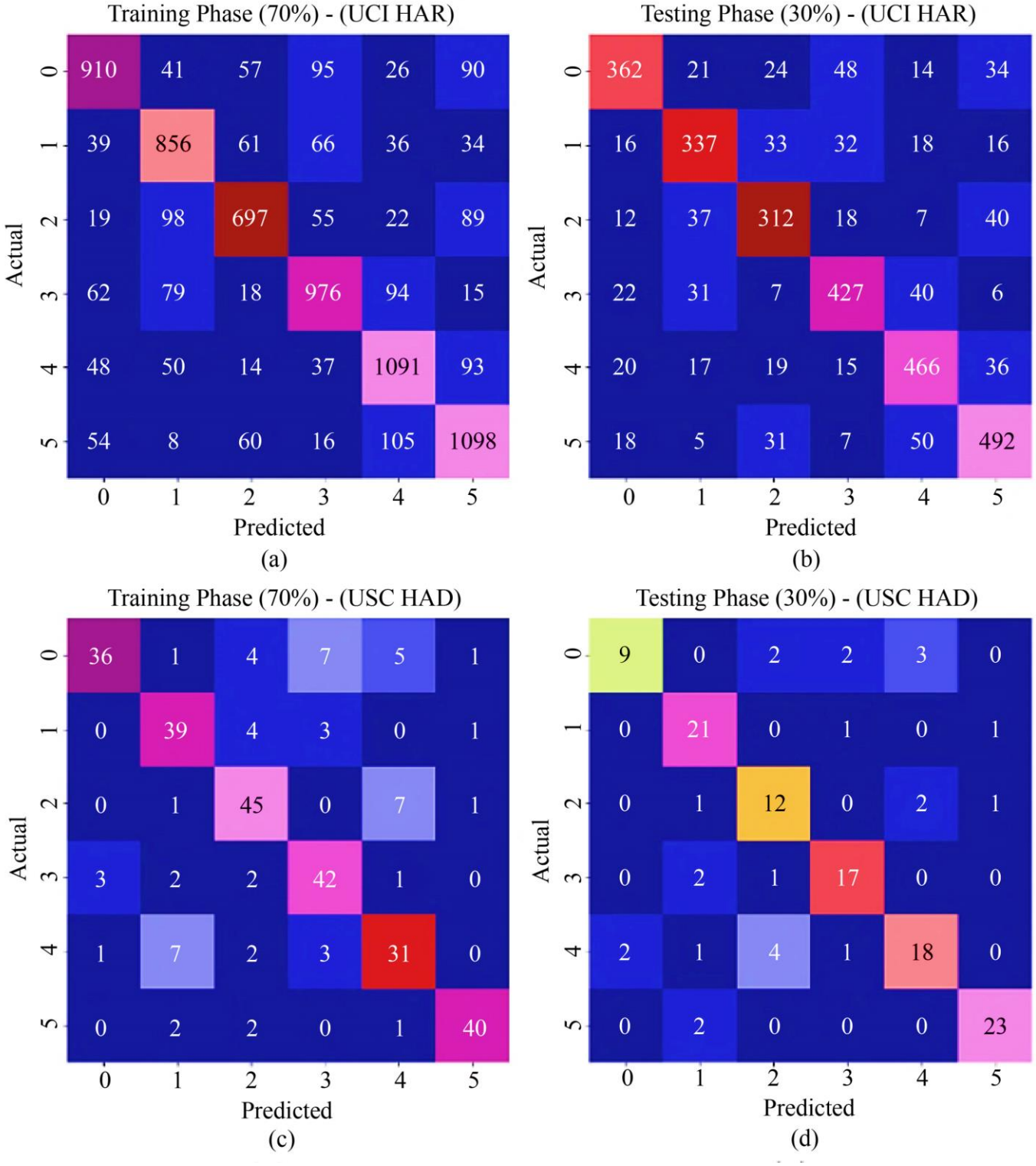

Fig. 3. Confusion matrix of (a-b) and (c-d) TR and TS datasets of 70:30 under the two datasets

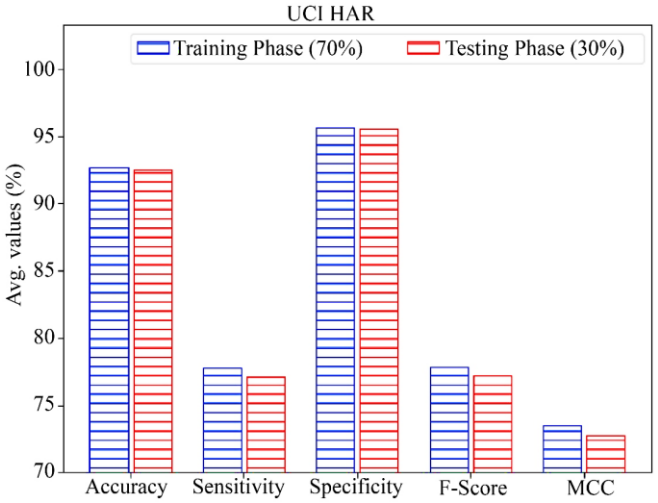

Fig. 4 Average investigation of the IMRFO-DAE model under the UCI HAR dataset

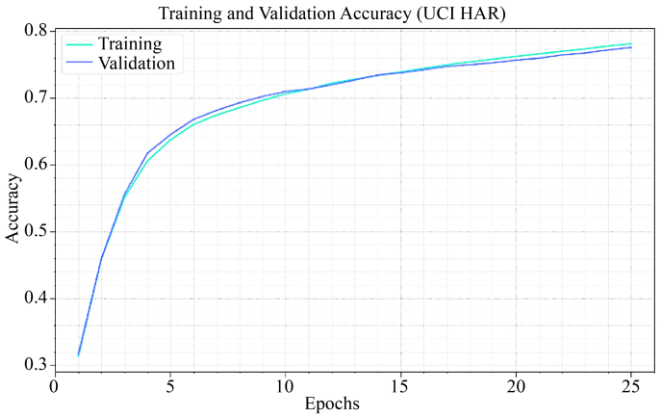

Fig. 5 TACC value and VACC value investigation of IMRFO-DAE method under UCI HAR dataset

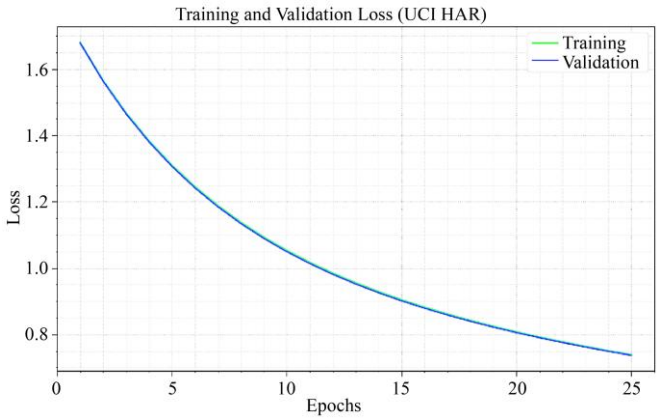

Fig. 6 TLS and VLS investigation of IMRFO-DAE method under UCI HAR dataset

The IMRFO-DAE model has identified all the human activities effectively on 70:30 percent of TR and TS datasets. For a sample, on 70% of the TR dataset, the IMRFO-DAE approach has gained an average $accu\_y$ of 92.69%, $sens\_y$ of 77.72%, $spec\_y$ of 95.60%, F_score of 77.81%, and MCC of 73.46%. Also, on 30% of the TS dataset, the IMRFO-DAE v has gained an average $accu\_y$ of 92.51%, $sens\_y$ of 77.13%, $spec\_y$ of 95.50%, F_score of 77.19%, and MCC of 72.73%. The TACC value and VACC value of the IMRFO-DAE methodology under the UCI HAR dataset examined on HAR achievement in Fig. 5. The figure signifies the IMRFO-DAE methodology has demonstrated an upgraded achievement with improved TACC value and VACC value.

The TLS value and VLS value of the IMRFO-DAE model under the UCI HAR dataset on HAR achievement are in Fig. 6.

The figure showed that the IMRFO-DAE method had improved achievement with the lowest TLS and VLS values. A detailed ROC analysis of the IMRFO-DAE methodology on a dataset of UCI HAR is shown in Fig. 7. The outcome stated that the IMRFO-DAE model has revealed its capacity to categorize various classes.

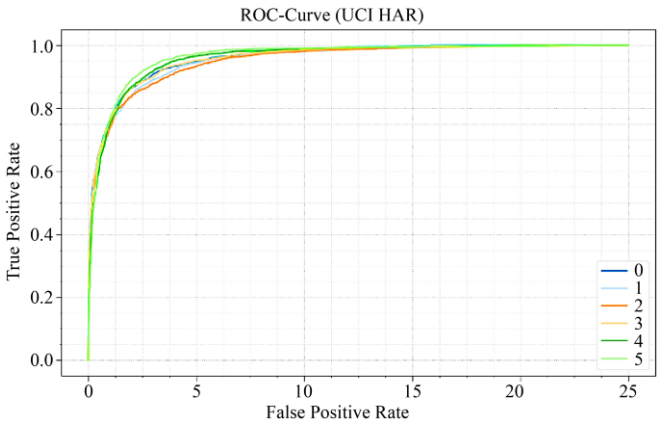

Fig. 7 ROC curve analysis of IMRFO-DAE approach under UCI HAR dataset

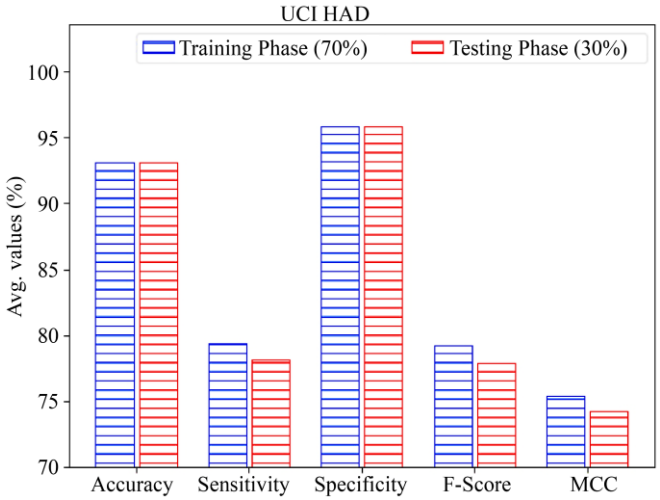

Fig. 8 Average analysis of the IMRFO-DAE approach in the USC HAD dataset

Table 4. HAR output of IMRFO-DAE model with distinct classes under USC HAD dataset

Labels	$Accu_y$	$Sens_y$	$Spec_y$	F_{Score}	MCC
Training (70%)					
0	92.52	66.67	98.33	76.60	73.41
1	92.86	82.98	94.74	78.79	74.64
2	92.18	83.33	94.17	79.65	74.93
3	92.86	84.00	94.67	80.00	75.79
4	90.82	70.45	94.40	69.66	64.26
5	97.28	88.89	98.80	90.91	89.34
Average	**93.08**	**79.39**	**95.85**	**79.27**	**75.40**
Testing (30%)					
0	92.86	56.25	98.18	66.67	64.20
1	93.65	91.30	94.17	84.00	80.47
2	91.27	75.00	93.64	68.57	63.86
3	94.44	85.00	96.23	82.93	79.65
4	89.68	69.23	95.00	73.47	67.29
5	96.83	92.00	98.02	92.00	90.02
Average	**93.12**	**78.13**	**95.87**	**77.94**	**74.25**

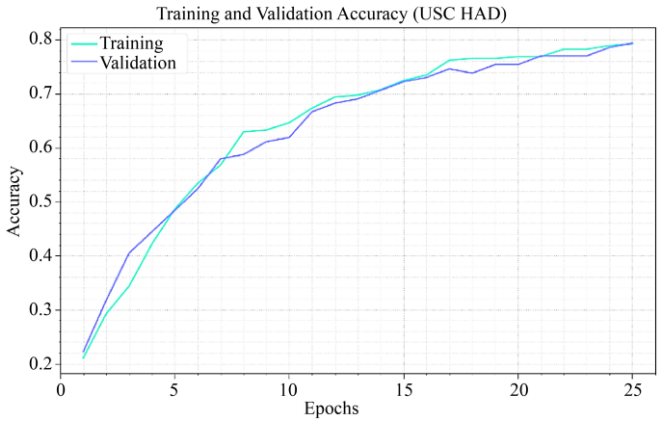

Fig. 9 TACC and VACC investigation of IMRFO-DAE model in the USC HAD dataset

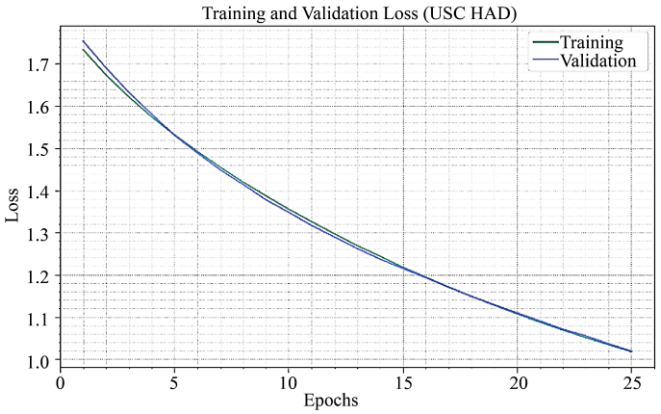

Fig. 10 TLS and VLS investigation of IMRFO-DAE model under USC HAD dataset

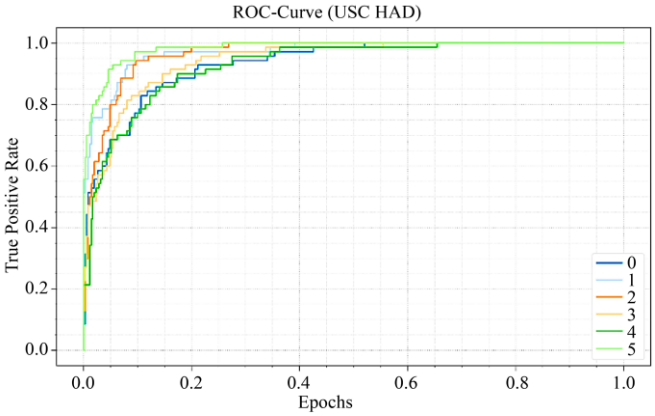

Fig. 11 ROC curve analysis of IMRFO-DAE approach under USC HAD dataset

Table 4 and Fig. 8 represent a comprehensive HAR outcome of the IMRFO-DAE algorithm on the USC HAD dataset.

The IMRFO-DAE approach has efficiently identified all human activities on 70:30 percent of TS datasets. For example, on 70% of the TR dataset, the IMRFO-DAE system has accomplished average $accu_y$ of 93.08%, $sens_y$ of 79.39%, $spec_y$ of 95.85%, F_{score} of 7927%, and MCC of 75.40%. Besides, on 30% of the TS dataset, the IMRFO-DAE approach has gained average $accu_y$ of 93.12%, $sens_y$ of 78.13%, $spec_y$ of 95.87%, F_{score} of 77.94%, and MCC of 74.25%.

The TACC value and VACC value of the IMRFO-DAE model under the USC HAD dataset are examined on HAR achievement in Fig. 9. The figure depicted that the IMRFO-DAE model has shown an upgraded achievement with the highest TACC value and VACC value. It is depicted that the IMRFO-DAE methodology has gained higher TACC outputs. The values of TLS and VLS of the IMRFO-DAE algorithm under the USC HAD database on HAR achievement in Fig. 10. The figure represented that the IMRFO-DAE methodology has exhibited an improved achievement with lower TLS and VLS values. It is evident that the IMRFO-DAE algorithm has given an outcome to lower VLS outputs.

A comprehensive ROC examination of the IMRFO-DAE algorithm on the USC HAD dataset is illustrated in Fig. 11. The output denoted the IMRFO-DAE approach has outperformed its capacity in categorizing in various classes.

Table 5 gives a comprehensive relational study of the IMRFO-DAE model with other DL approaches. Fig. 12 presents comparative results of the IMRFO-DAE model on the UCI HAR dataset. The simulation outcome denoted that the CNN-LSTM system has depicted a lower $accu\_y$ of 87.339%. Along with that, the CNN and LSTM methods have revealed certainly enhanced $accu\_y$ of 89.456% and 89.674%

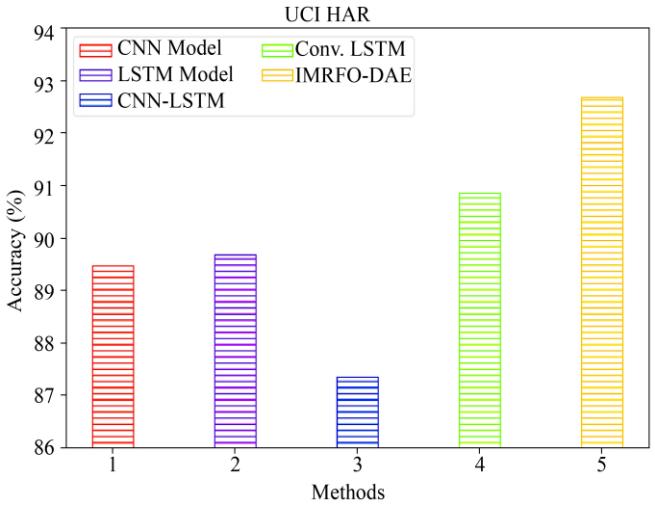

Fig. 12 Comparative analysis of IMRFO-DAE approach under the UCI HAR dataset

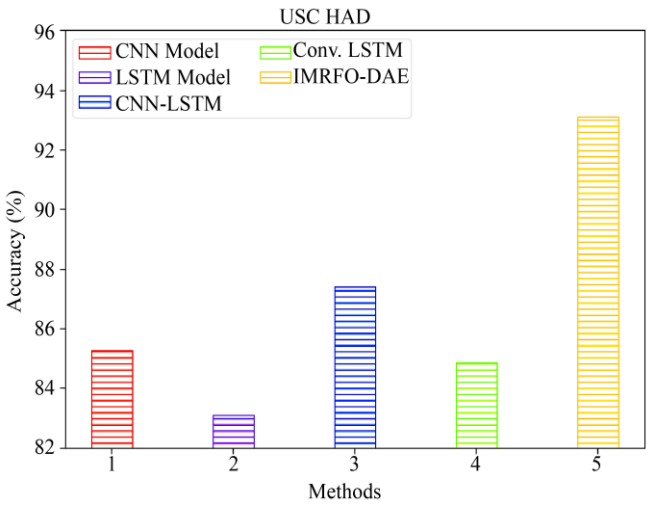

Fig. 13. Comparative investigation of the IMRFO-DAE method under the USC HAD dataset

Table 5. Comparative investigation of the IMRFO-DAE model with other models under the UCI HAR dataset and USC HAD dataset

Models	UCI HAR	USC HAD
CNN	89.456	85.264
LSTM	89.674	83.084
CNN-LSTM	87.339	87.414
Conv. LSTM	90.851	84.862
IMRFO-DAE	92.690	93.120

-subsequently. Although the Conv-LSTM model has reported near optimal $accu_y$ of 90.851%, the IMRFO-DAE model exhibited its supremacy with maximum $accu_y$ of 92.690%.

Fig. 13 offers a comparative outcome of the IMRFO-DAE approach on the USC HAD database.

The simulation outcome referred that the LSTM system has revealed lesser $accu_y$ of 83.084%. Followed by the Conv-LSTM and CNN systems have exposed certainly greater $accu_y$ of 84.862% and 85.264%, respectively. But, the CNN-LSTM model has reported near optimum $accu_y$ of 87.414%, the IMRFO-DAE algorithm displayed its supremacy with superior $accu_y$ of 93.12%. These outputs demonstrate the improved achievement of the IMRFO-DAE approach.

4. Conclusion

In the present study, a novel IMRFO-DAE algorithm for accurate HAR. The presented IMRFO-DAE algorithm majorly recognized the diverse classes of human activities. The presented model pre-processed the human activity data via a standardization approach to obtain this.

Then, the IMRFO-DAE algorithm performs the AR process using the DAE model. For enhancing the activity detection performance of the DAE algorithm, the IMRFO algorithm is applied as a hyperparameter optimizer.

Moreover, the IMRFO model is derived by modifying the initialization of the MRFO model utilizing the chaotic concept. An extensive range of simulations were carried out to demonstrate the enhanced performance of the IMRFO-DAE system.

The simulation results assured the improved outcomes of the IMRFO-DAE approach compared to existing approaches. In the future, the deep ensemble fusion algorithm can be employed to optimize the recognition performance.

References

[1] Anindita Saha et al., "A Survey of Machine Learning and Meta-heuristics Approaches for Sensor-based Human Activity Recognition Systems," *Journal of Ambient Intelligence and Humanized Computing*, pp. 1-28, 2022. [CrossRef] [Google Scholar] [Publisher Link]

[2] Maninder Kaur et al., "Binary Cuckoo Search Metaheuristic-based Supercomputing Framework for Human Behavior Analysis in Smart Home," *The Journal of Supercomputing*, vol. 76, no. 4, pp. 2479-2502, 2020. [CrossRef] [Google Scholar] [Publisher Link]

[3] HritamBasak et al., "A Union of Deep Learning and Swarm-Based Optimization for 3D Human Action Recognition," *Scientific Reports*, vol. 12, no. 1, pp.1-17, 2022. [CrossRef] [Google Scholar] [Publisher Link]

[4] Henry Friday Nweke et al., "Multi-Sensor Fusion Based on Multiple Classifier Systems for Human Activity Identification," *Human-Centric Computing and Information Sciences*, vol. 9, no. 1, pp. 1-44, 2019. [CrossRef] [Google Scholar] [Publisher Link]

[5] Çağatay Berke Erdaş, and Selda Güney, "Human Activity Recognition by Using Different Deep Learning Approaches for Wearable Sensors," *Neural Processing Letters*, vol. 53, no. 3, pp. 1795-1809, 2021. [CrossRef] [Google Scholar] [Publisher Link]

[6] Tengyue Li et al., "Fusing Wearable and Remote Sensing Data Streams by Fast Incremental Learning with Swarm Decision Table for Human Activity Recognition," *Information Fusion*, vol. 60, pp. 41-64, 2020. [CrossRef] [Google Scholar] [Publisher Link]

[7] Türker Tuncer, and Fatih Ertam, "Novel Tent Pooling Based Human Activity Recognition Approach," *Multimedia Tools and Applications*, vol. 80, no. 3, pp. 4639-4653, 2021. [CrossRef] [Google Scholar] [Publisher Link]

[8] C. Nithyeswari, and G. Karthikeyan, "An Ensemble of Deep Learning with Optimization Model for Activity Recognition in the Internet of Things Environment," *SSRG International Journal of Electrical and Electronics Engineering*, vol. 10, no. 4, pp. 91-104, 2023. [CrossRef] [Google Scholar] [Publisher Link]

[9] Stefan Tsokov, Milena Lazarova, and Adelina Aleksieva-Petrova, "Evolving 1d Convolutional Neural Networks for Human Activity Recognition," *International Conference on Computer Systems and Technologies*, vol. 21, pp. 49-54, 2021. [CrossRef] [Google Scholar] [Publisher Link]

[10] Hongqing Fang, Pei Tang, and Hao Si, "Feature Selections using Minimal Redundancy Maximal Relevance Algorithm for Human Activity Recognition in Smart Home Environments," *Journal of Healthcare Engineering*, 2020. [CrossRef] [Google Scholar] [Publisher Link]

[11] Abdelghani Dahou et al., "Human Activity Recognition in the Internet of Things Applications using Arithmetic Optimization Algorithm and Deep Learning," *Measurement*, vol. 199, 2022. [CrossRef] [Google Scholar] [Publisher Link]

[12] Anand Upadhyay et al., "Body Posture Detection using Computer Vision," *SSRG International Journal of VLSI & Signal Processing*, vol. 7, no. 1, pp. 6-10, 2020. [CrossRef] [Publisher Link]

[13] Changjun Fan, and Fei Gao, "Enhanced Human Activity Recognition using Wearable Sensors Via a Hybrid Feature Selection Method, " *Sensors*, vol. 21, no. 19, p. 6434, 2021. [CrossRef] [Google Scholar] [Publisher Link]

[14] Muhammad Attique Khan et al., "Traditional Features based Automated System for Human Activities Recognition," *2nd International Conference on Computer and Information Sciences*, pp. 1-6, 2020. [CrossRef] [Google Scholar] [Publisher Link]

[15] Devang Jani, and Anand Mankodia, "A Novel Approach for Real Time Multi-Scene Violent Activities Recognition with Modified ResNet50 and LSTM," *International Journal of Engineering Trends and Technology*, vol. 70, no. 8, pp. 292-309, 2022. [CrossRef] [Publisher Link]

[16] Ahmed Mohamed Helmi et al., "A Novel Hybrid Gradient-Based Optimizer and Grey Wolf Optimizer Feature Selection Method for Human Activity Recognition using Smartphone Sensors," *Entropy*, vol. 23, no. 8, 2021. [CrossRef] [Google Scholar] [Publisher Link]

[17] H S Shreenidhi, and Narayana Swamy Ramaiah, "Sensor-Assisted Machine Learning Models Approach to Equipoise Renewable Energy using Microgrids," *SSRG International Journal of Electronics and Communication Engineering*, vol. 10, no. 7, pp. 63-73, 2023. [CrossRef] [Publisher Link]

[18] Emad M. Ahmed et al., "Modified Manta-Ray Foraging Optimization Algorithm Based Improved Load Frequency Controller for Interconnected Microgrids," *IET Renewable Power Generation*, 2022. [CrossRef] [Google Scholar] [Publisher Link]

[19] Human Activity Recognition Using Smartphones, 2012. [Online]. Available: https://archive.ics.uci.edu/ml/datasets/human+activity+recognition+using+smartphones

[20] The USC-SIPI Human Activity Dataset, 2012. [Online]. Available: http://sipi.usc.edu/had/

[21] L. Maria Anthony Kumar, S. Murugan, and A. Therasa Alphonsa, "Robust Human Activity Recognition using Equilibrium Optimizer with Deep Extreme Learning Machine Model," *SSRG International Journal of Electrical and Electronics Engineering*, vol. 10, no. 5, pp. 1-13, 2023. [CrossRef] [Publisher Link]

[22] Samanta Rosati, Gabriella Balestra, and Marco Knaflitz, "Comparison of Different Sets of Features for Human Activity Recognition by Wearable Sensors," *Sensors*, vol. 18, no. 12, p. 4189, 2018. [CrossRef] [Google Scholar] [Publisher Link]

[23] Saeid Raziani, and Mehran Azimbagirad, "Deep Convolutional Neural Networks Hyperparameter Optimization Algorithms for Sensor-based Human Activity Recognition," *Neuroscience Informatics*, vol. 2, no. 3, 2022. [CrossRef] [Google Scholar] [Publisher Link]

[24] Zhiyi He et al., "Modified Deep Autoencoder Driven by Multisource Parameters for Fault Transfer Prognosis of Aeroengine," *IEEE Transactions on Industrial Electronics*, vol. 69, no. 1, pp. 845-855, 2021. [CrossRef] [Google Scholar] [Publisher Link]

[25] Fahd N. Al-Wesabi et al., "Design of Optimal Deep Learning Based Human Activity Recognition on Sensor Enabled Internet of Things Environment," *IEEE Access*, vol. 9, pp.143988-143996, 2021. [CrossRef] [Google Scholar] [Publisher Link]